Inorg. Chem. **2003**, *42*, 6989–6995

Exploration of Composition Space in Templated Uranium Sulfates

Michael B. Doran, Alexander J. Norquist,† and Dermot O'Hare*

Inorganic Chemistry Laboratory, University of Oxford, South Parks Road, Oxford OX1 3QR, U.K.

Received May 19, 2003

The phase stability of organically templated uranium sulfates in the $[UO_2(CH_3CO_2)_2 \cdot 2H_2O$/homopiperazine/$H_2SO_4]$ and $[UO_2(CH_3CO_2)_2 \cdot 2H_2O$/*N*,*N*-dimethylethylenediamine/$H_2SO_4]$ systems has been studied using composition space. Two new compounds were formed in each system; $[N_2C_5H_{14}]_2[UO_2(SO_4)_3]$ (USO-17) and $[N_2C_5H_{14}][UO_2(H_2O)(SO_4)_2]$ (USO-18) contain homopiperazine, and $[N_2C_4H_{14}][UO_2(SO_4)_2]$ (USO-19) and $[N_2C_4H_{14}][(UO_2)_2(H_2O)(SO_4)_3] \cdot H_2O$ (USO-20) contain *N*,*N*-dimethylethylenediamine. The relative stability of the products from each system is dependent upon the reactant mole fractions in the initial reaction gel. Crystal data: USO-17, $a = 14.4975(3)$ Å, $b = 11.9109(3)$ Å, $c = 13.0157(3)$ Å, $\beta = 110.475(1)°$, monoclinic, *C*2/*c* (No. 15), $Z = 4$; for USO-18, $a = 7.6955(2)$ Å, $b = 11.7717(3)$ Å, $c = 14.7038(4)$ Å, orthorhombic, $P22_12_1$ (No. 18), $Z = 4$; for USO-19, $a = 9.3322(1)$ Å, $b = 9.7743(2)$ Å, $c = 13.8897(3)$ Å, orthorhombic, $P2_12_12_1$ (No. 19), $Z = 4$; and for USO-20, $a = 11.2460(2)$ Å, $b = 10.5387(2)$ Å, $c = 17.0432(3)$ Å, $\beta = 92.9884(6)°$, monoclinic, $P2_1/c$ (No. 14), $Z = 4$.

Introduction

Hydrothermal synthesis is a well-established method for the formation of inorganic structures templated by organic ions. The majority of these compounds are metal phosphates,[1] with other examples including metal phosphites,[2] fluorides,[3] germanates,[4] arsenates,[5] oxalates,[6] and selenites.[7]

A recently employed strategy for the design of new inorganic architectures involves the use of the sulfate tetrahedron as a primary substituent.[8] The preparation of organically templated metal sulfates is of interest for several reasons. First, the $[SO_4]^{2-}$ tetrahedron is approximately the same size and shape as $[PO_4]^{3-}$. However, the difference in charge can result in the formation of new structural assemblies. Second, the majority of reports detailing the preparation of templated metal sulfates have occurred in the past two years. This area is underexplored with respect to phosphate chemistry. Third, great structural diversity is exhibited in the small set of reported metal sulfates. The existence of compounds containing inorganic components whose dimensionalities range from zero-dimensional molecular anions to three-dimensional microporous frameworks suggests that many new structure types can be discovered.

One method employed by researchers to gain understanding in hydrothermal reactions is the use of composition space.[9] Composition space involves the introduction of subtle

* To whom correspondence should be addressed. E-mail: dermot.ohare@chem.ox.ac.uk.

† Current address: Department of Chemistry, Haverford College, Haverford, PA 19041.

(1) Cheetham, A. K.; Férey, G.; Loiseau, T. *Angew. Chem., Int. Ed.* **1999**, *38*, 3268.

(2) (a) Doran, M.; Walker, S. M.; O'Hare, D. *Chem. Commun.* **2001**, 1988. (b) Fernandez, S. J.; Mesa, L.; Pizarro, J. L.; Lezama, L.; Arriortura. M. I.; Rojo, T. *Chem. Mater.* **2002**, *14*, 2300.

(3) Walker, S. M.; Halasyamani, P. S.; O'Hare, D. *J. Am. Chem. Soc.* **1999**, *121*, 7415.

(4) (a) Reisner, B. A.; Tripathi, A.; Parise, J. B. *J. Mater. Chem.* **2001**, *11*, 887. (b) Bu, X.; Feng, P.; Gier, T. E.; Zhao, D.; Stucky, G. D. *J. Am. Chem. Soc.* **1998**, *120*, 13389. (c) Conradsson, T.; Zou, X.; Dadachov, M. *Inorg. Chem.* **2000**, *39*, 1716.

(5) (a) Ekambarem, S.; Sevov, S. *Inorg. Chem.* **2000**, *39*, 2405. (b) Bazan, B.; Mesa, J. L.; Pizarro, J. L.; Lezama, L.; Arriorturaand, M. I.; Rojo, T. *Inorg. Chem.* **2000**, *39*, 6056.

(6) Vaidhyanathan, R.; Natarajan, S.; Rao, C. N. R. *Inorg. Chem.* **2002**, *17*, 4496.

(7) (a) Choudhury, A.; Kumar, U.; Rao, C. N. R. *Angew. Chem., Int. Ed.* **2002**, *41*, 158. (b) Harrison, W. T. A.; Phillips, M. L. F.; Stanchfield, J.; Nenoff, T. M. *Angew. Chem., Int. Ed.* **2000**, *39*, 3808.

(8) (a) Choudhury, A.; Krishnamoorthy, J.; Rao, C. N. R. *Chem. Commun.* **2001**, 2610. (b) Paul, G.; Choudhury, A.; Rao, C. N. R. *J. Chem. Soc., Dalton Trans.* **2002**, 3859. (c) Thomas, P. M.; Norquist, A. J.; Doran, M. B.; O'Hare D. *J. Mater. Chem.* **2003**, *13*, 88. (d) Norquist, A. J.; Thomas, P. M.; Doran, M. B.; O'Hare, D. *Chem. Mater.* **2002**, *14*, 5179. (e) Doran, M. B.; Norquist, A. J.; O'Hare, D. *Chem. Commun.* **2002**, 2946. (f) Norquist, A. J.; Doran, M. B.; Thomas, P. M.; O'Hare D. *J. Chem. Soc., Dalton Trans.* **2003**, 1168. (g) Norquist, A. J.; Doran, M. B.; O'Hare, D. *Solid State Sci.* **2003**, *8*, 1149. (h) Paul, G.; Choudhury, A.; Rao, C. N. R. *Chem. Commun.* **2002**, 1904. (i) Paul, G.; Choudhury, A.; Sampathkumaran, E. V.; Rao, C. N. R. *Angew. Chem., Int. Ed.* **2002**, *41*, 4297. (j) Paul, G.; Choudhury, A.; Rao, C. N. R. *Chem. Mater.* **2003**, *15*, 1174. (k) Paul, G.; Choudhury, A.; Nagarajan, R.; Rao, C. N. R. *Inorg. Chem.* **2003**, *42*, 2004. (l) Khan, M. I.; Cevik, S.; Doedens, R. J. *Inorg. Chim. Acta* **1999**, *292*, 112. (m) Bataille, T.; Louër, D. *J. Mater. Chem.* **2002**, *12*, 3487. (n) Xing, Y.; Shi, Z.; Li, G.; Pang, W. *J. Chem. Soc., Dalton Trans.* **2003**, 940. (o) Wang, D.; Yu, R.; Xu, Y.; Feng, S.; Xu, R.; Kumada, N.; Kinomura, N.; Matsumura, Y.; Takano, M. *Chem. Lett.* **2002**, 1120. (p) Bull, I.; Wheatley, P. S.; Lightfoot, P.; Morris, R. E.; Sastre, E.; Wright, P. A. *Chem. Commun.* **2002**, 1180. (q) Doran, M. B.; Norquist, A. J.; O'Hare, D. *Acta Crystallogr., Sect. E* **2003**, *59*, m373−m375. (r) Stuart, C. L.; Doran, M. B.; Norquist, A. J.; O'Hare, D. *Acta Crystallogr., Sect. E* **2003**, *59*, m446−m448.

10.1021/ic034540j CCC: $25.00
Published on Web 10/04/2003

variations in reactant concentrations over a series of analagous experiments. All other reaction variables such as temperature, solvent concentration, and reaction time are held constant. This enables the direct observation of the effects that result from differences in reactant concentrations. Composition space can be used to isolate reaction variables in complex hydrothermal reactions.

Composition space diagrams have been constructed in the [UO_2Ac_2·$2H_2O$/homopiperazine/H_2SO_4] and [UO_2Ac_2·$2H_2O$/*N*,*N*-dimethylethylenediamine/H_2SO_4] systems (Ac = $CH_3CO_2^-$) and the factors governing phase stability of the crystalline products elucidated. Four new organically templated uranium sulfates are reported. These materials are designated USO-17, USO-18, USO-19, and USO-20 (uranium sulfate from Oxford).

Experimental Section

Caution. Although all uranium materials used in these experiments were depleted, extra care and good laboratory practice should always be used when handling uranium containing materials.

Materials. Homopiperazine (98%, Aldrich), *N*,*N*-dimethylethylenediamine (95%, Aldrich), and sulfuric acid (98%, Aldrich) were used as received. Deionized water was used in these syntheses. UO_2Ac_2·$2H_2O$ was prepared[10] from UO_3 (99.8%, Strem).

Synthesis. All reactions were conducted in poly(fluoro-ethylene-propylene) lined 23 mL stainless steel autoclaves. Reactions were heated to 180 °C at 10 °C min^{-1}, where the temperature was held constant for 24 h. The reactions were cooled to room temperature at 6 °C h^{-1} and the autoclaves opened in air. Solid products were recovered using filtration and washed with deionized water and acetone.

$[N_2C_5H_{14}]_2[UO_2(SO_4)_3]$ (USO-17) was synthesized through the reaction of 0.1374 g (3.24×10^{-4} mol) of UO_2Ac_2·$2H_2O$, 0.2671 g (2.72×10^{-3} mol) of H_2SO_4, 0.2275 g (2.27×10^{-3} mol) of hpip (homopiperazine), and 1.0117 g (5.62×10^{-2} mol) of deionized water. Yellow rods were isolated after reaction in a yield of 84%. Elemental microanalysis for USO-17 obsd (calcd): N, 7.33 (7.35); C, 15.95 (15.75); H, 3.72 (3.70); S, 13.08 (12.62); U, 29.96% (31.21%). $[N_2C_5H_{14}][UO_2(H_2O)(SO_4)_2]$ (USO-18) was synthesized through the reaction of 0.1067 g (2.52×10^{-4} mol) of UO_2Ac_2·$2H_2O$, 0.3889 g (3.96×10^{-3} mol) of H_2SO_4, 0.0893 g (8.92×10^{-4} mol) of homopiperazine, and 1.0218 g (5.68×10^{-2} mol) of deionized water. Yellow blocks were isolated after reaction in a yield of 77%. Elemental microanalysis for USO-18 obsd (calcd): N, 4.90 (4.81); C, 10.48 (10.31); H, 3.10 (2.70); S, 12.70 (11.01); U, 39.47% (40.87%). $[N_2C_4H_{14}][UO_2(SO_4)_2]$ (USO-19) was synthesized through the reaction of 0.1168 g (2.75×10^{-4} mol) of UO_2Ac_2·$2H_2O$, 0.4102 g (4.19×10^{-3} mol) of H_2SO_4, 0.0714 g (8.12×10^{-4} mol) of dmed (*N*,*N*-dimethylethylenediamine), and 0.5087 g (2.83×10^{-2} mol) of deionized water. Yellow blocks were isolated after reaction in a yield of 55%. Elemental microanalysis for USO-19 obsd (calcd): N, 5.03 (5.07); C, 8.82 (8.70); H, 2.44 (2.55); S, 13.33 (11.61); U, 41.44% (43.10%). $[N_2C_4H_{14}]$-$[(UO_2)_2(H_2O)(SO_4)_3]$·H_2O (USO-20) was synthesized through the reaction of 0.3155 g (7.44×10^{-4} mol) of UO_2Ac_2·$2H_2O$, 0.4219 g (4.31×10^{-3} mol) of H_2SO_4, 0.0854 g (9.71×10^{-4} mol) of *N*,*N*-dimethylethylenediamine, and 0.5134 g (2.85×10^{-2} mol) of deionized water. Yellow blocks were isolated after reaction in a yield of 67%. Elemental microanalysis for USO-20 obsd (calcd): N, 3.02 (2.94); C, 5.12 (5.03); H, 2.17 (1.90); S, 11.56 (10.01); U, 49.76% (49.88%).

Powder X-ray diffraction patterns of each bulk sample match the pattern generated from the respective single-crystal X-ray structure data.

X-ray Crystallographic Analysis. Single crystals of each compound were used for structure determination. Data were collected using an Enraf Nonius FR 590 Kappa CCD diffractometer with graphite monochromated Mo Kα radiation ($\lambda = 0.71073$ Å). Crystals were mounted on a glass fiber using N-Paratone oil and cooled in-situ using an Oxford Cryostream 600 Series to 150 K for data collection. Frames were collected, indexed, and processed using Denzo SMN and the files scaled together using HKL GUI within Denzo SMN.[11] The heavy atom positions were determined using SIR97.[12] All other non-hydrogen sites were located from Fourier difference maps. All non-hydrogen sites were refined using anisotropic thermal parameters using full-matrix least-squares procedures on F_o^2 with $I > 3\sigma(I)$. Hydrogen atoms were placed in geometrically idealized positions. All calculations were performed using Crystals[13] and Cameron.[14] Relevant crystallographic data are listed in Table 1, and selected bond lengths are listed in Tables 2−5.

Powder X-ray Diffraction. Powder X-ray diffraction patterns were recorded on a Philips PW 1729 diffractometer. Samples were mounted on aluminum plates. Calculated powder patterns were generated from the single crystal data using the computer program ATOMS.[15]

Infrared Spectroscopy. All infrared measurements were obtained using a Perkin-Elmer 1600 FT spectrometer. Samples were diluted with spectroscopic KBr and pressed into a pellet. Scans were run over the range 400−4000 cm^{-1}.

Elemental Analysis. C, H, and N analyses were conducted using an Elementar Vario EL analyzer. S and U compositions were determined by ICP using a Thermo Jarrell Ash Scan 16 instrument.

Thermogravimetric Analysis. TGA measurements were performed on a Rheometric Scientific STA 1500H thermal analyzer. The samples were loaded into an alumina crucible and heated at 10 °C min^{-1} under flowing argon. See Supporting Information for TGA traces.

Results

The coordination of the U^{6+} center in each of the reported compounds is similar. Each uranium center is bound to two axial oxides forming a uranyl unit, $[UO_2]^{2+}$. The $U-O_{uranyl}$ bond lengths range between 1.758(5) and 1.785(3) Å, in good agreement with the reported average uranyl bond length of 1.758(4) Å.[16] The uranyl unit in USO-17 is coordinated to

(9) (a) Halasyamani, P. S.; Willis, M. J.; Stern, C. L.; Lundquist, P. M.; Wong, G. K.; Poeppelmeier, K. R. *Inorg. Chem.* **1996**, *35*, 1367. (b) Harrison, W. T. A.; Dussack, L. L.; Jacobson, A. J. *J. Solid State Chem.* **1996**, *125*, 234. (c) Norquist, A. J.; Heier, K. R.; Stern, C. L.; Poeppelmeier, K. R. *Inorg. Chem.* **1998**, *37*, 6495.
(10) Halasyamani, P. S.; Francis, R. J.; Walker, S. M.; O'Hare, D. *Inorg. Chem.* **1999**, *38*, 271.
(11) Otwinowski, Z. *Data Collection and Processing*; Daresbury Laboratory: Warrington, U.K., 1993.
(12) Cascarano, G.; Giacovazzo C.; Guagliardi, A. *J. Appl. Crystallogr.* **1993**, *26*, 343.
(13) Watkin, D. J.; Prout, C. K.; Carruthers, J. R.; Betteridge, P. W.; Cooper, R. I. *CRYSTALS Issue 11*; Chemical Crystallography Laboratory: Oxford, U.K., 2001.
(14) Watkin, D. J.; Prout, C. K.; Pearce, L. J. *CAMERON*; Chemical Crystallography Laboratory: Oxford, U.K., 1996.
(15) Dowty, E. *ATOMS* v. 5.0.7; Shape Software: Kingsport, TN.
(16) Burns, P. C.; Ewing, R. C.; Hawthorne, F. C. *Can. Mineral.* **1997**, *35*, 1551.

Table 1. Crystallographic Data

compd	USO-17	USO-18	USO-19	USO-20
formula	$[N_2C_5H_{14}]_2$-$[UO_2(SO_4)_3]$	$[N_2C_5H_{14}][UO_2$-$(H_2O)(SO_4)_2]$	$[N_2C_4H_{14}]$-$[UO_2(SO_4)_2]$	$[N_2C_4H_{14}][(UO_2)_2$-$(H_2O)(SO_4)_3]\cdot H_2O$
fw	762.57	582.35	552.32	954.45
space group	*C*2/*c* (No. 15)	$P22_12_1$ (No. 18)	$P2_12_12_1$ (No. 19)	$P2_1/c$ (No. 14)
a/Å	14.4975(3)	7.6955(2)	9.3322(1)	11.2460(2)
b/Å	11.9109(3)	11.7717(3)	9.7743(2)	10.5387(2)
c/Å	13.0157(3)	14.7038(4)	13.8897(3)	17.0432(3)
α/deg	90	90	90	90
β/deg	110.475(1)	90	90	92.9884(6)
γ/deg	90	90	90	90
V/Å^3	2105.54(8)	1332.00(6)	1266.96(4)	2017.18(6)
Z	4	4	4	4
ρ_{calcd}/g cm^{-3}	2.405	2.904	2.895	3.143
T/K	150	150	150	150
λ/Å	0.71073	0.71073	0.71073	0.71073
μ/mm^{-1}	8.086	12.561	13.192	16.434
$R(F_o)^a$	0.0242	0.0268	0.0227	0.0265
$R_w(F_o^2)^b$	0.0524	0.0675	0.0560	0.0635

^{a} $R = \sum||F_o| - |F_c||/\sum|F_o|$. ^{b} $R_w = [\sum w(|F_o^2| - |F_c^2|)^2/\sum w(F_o^2)^2]^{1/2}$.

Table 2. Selected Bond Lengths (Å) for USO-17

U(1)−O(1)	1.785(3)	S(2)−O(3)	1.506(3)
U(1)−O(2)	2.447(3)	S(2)−O(4)	1.520(3)
U(1)−O(3)	2.464(3)	S(2)−O(6)	1.441(3)
U(1)−O(4)	2.452(3)	S(2)−O(7)	1.453(3)
S(1)−O(2)	1.528(3)		
S(1)−O(5)	1.444(3)		

Table 3. Selected Bond Lengths (Å) for USO-18

U(1)−O(1)	1.777(4)	U(2)−O(5)	1.781(4)
U(1)−O(2)	2.463(7)	U(2)−O(6)	2.465(7)
U(1)−O(3)	2.346(4)	U(2)−O(7)	2.345(4)
U(1)−O(4)	2.362(4)	U(2)−O(8)	2.373(4)
S(1)−O(4)	1.502(6)	S(2)−O(3)	1.497(6)
S(1)−O(7)	1.483(7)	S(2)−O(8)	1.482(5)
S(1)−O(9)	1.468(5)	S(2)−O(11)	1.464(5)
S(1)−O(10)	1.439(6)	S(2)−O(12)	1.452(5)

Table 4. Selected Bond Lengths (Å) for USO-19

		S(1)−O(3)	1.497(4)
U(1)−O(1)	1.775(3)	S(1)−O(4)	1.494(4)
U(1)−O(2)	1.777(3)	S(1)−O(8)	1.454(4)
U(1)−O(3)	2.312(4)	S(1)−O(9)	1.452(5)
U(1)−O(4)	2.311(3)		
U(1)−O(5)	2.467(4)	S(2)−O(5)	1.490(4)
U(1)−O(6)	2.507(4)	S(2)−O(6)	1.486(4)
U(1)−O(7)	2.407(4)	S(2)−O(7)	1.485(4)
		S(2)−O(10)	1.458(4)

six oxide ligands in the equatorial plane, forming a hexagonal bipyramid. In USO-18, USO-19, and USO-20, the uranyl unit is coordinated to five equatorial oxides, forming pentagonal bipyramids. U−O_{eq} distances range between 2.311(3) and 2.507(4) Å. Bond valence calculations[17,18] on USO-17 through USO-20, using uranium parameters from Burns et al.,[16] resulted in values between 5.976 and 6.128. Each sulfur site in USO-17, USO-18, USO-19, and USO-20 is four coordinate in a tetrahedral geometry. S−O distances range between 1.439(5) and 1.528(3) Å.

USO-17. The inorganic structure and the three-dimensional packing are shown in Figure 1. One uranium site is observed in USO-17. The six equatorial coordination sites around each $[UO_2]^{2+}$ uranyl group are occupied by oxide ligands that are part of sulfate tetrahedra. Two sulfur environments exist in USO-17. Each sulfate tetrahedron shares an edge with the uranium polyhedron, forming a zero-dimensional molecular unit, $[UO_2(SO_4)_3]^{4-}$. A related anion has been observed in the mineral liebigite, $Ca_2[(UO_2)(CO_3)_3](H_2O)_{11}$.[19]

Table 5. Selected Bond Lengths (Å) for USO-20

U(1)−O(1)	1.767(5)	U(2)−O(8)	1.763(5)
U(1)−O(2)	1.765(5)	U(2)−O(9)	1.758(5)
U(1)−O(3)	2.376(5)	U(2)−O(10)	2.452(5)
U(1)−O(4)	2.370(5)	U(2)−O(11)	2.404(5)
U(1)−O(5)	2.458(5)	U(2)−O(12)	2.362(5)
U(1)−O(6)	2.328(5)	U(2)−O(13)	2.400(5)
U(1)−O(7)	2.365(5)	U(2)−O(14)	2.394(5)
S(1)−O(3)	1.501(5)	S(3)−O(7)	1.484(5)
S(1)−O(11)	1.477(5)	S(3)−O(12)	1.471(5)
S(1)−O(14)	1.481(5)	S(3)−O(13)	1.471(5)
S(1)−O(15)	1.439(5)	S(3)−O(16)	1.457(5)
S(2)−O(4)	1.491(5)		
S(2)−O(6)	1.481(5)		
S(2)−O(10)	1.490(5)		
S(2)−O(17)	1.441(5)		

The $[UO_2(SO_4)_3]^{4-}$ units are separated by protonated homopiperazine templates, $[hpipH_2]^{2+}$, with each moiety stacking along the [0 0 1] direction. The $[hpipH_2]^{2+}$ cations donate hydrogen bonds to the uranyl sulfate units, as well as balance charge. N(1) donates hydrogen bonds to O(2) and O(3) through distances of 2.906(7) and 2.884(7) Å. N(2) donates hydrogen bonds to O(4) and O(7) through distances of 2.803(7) and 2.764(7) Å, respectively.

The presence of the template is confirmed using infrared spectroscopy. N−H bands are observed between 2750 and 3250 cm^{-1}, and at 1612 cm^{-1}, together with C−H bands centered around 1460 cm^{-1}. S−O bands are observed between 1100 and 1250 cm^{-1}. The asymmetric uranyl stretch is observed at 905 cm^{-1}.

USO-17 is thermally stable up to 300 °C using thermogravimetric analysis. A two step weight loss occurs between 300 and 460 °C and 460 and 900 °C, corresponding to the loss of the template and decomposition of the inorganic structure. The material calcines to UO_2, as determined using

(17) Brown, I. D.; Altermatt, D. *Acta Crystallogr., Sect. B* **1985**, *41*, 244.
(18) Brese, N. E.; O'Keeffe, M. *Acta Crystallogr., Sect. B* **1991**, *47*, 192.
(19) Mereiter, K. *TMPM, Tschermaks Mineral. Petrogr. Mitt.* **1982**, *30*, 277−288.

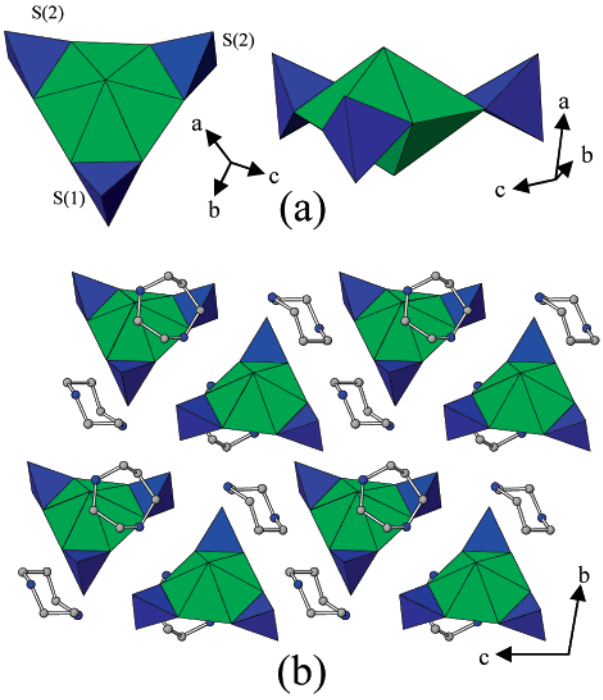

Figure 1. (a) Zero-dimensional $[UO_2(SO_4)_3]^{4-}$ molecules in USO-17. (b) Three-dimensional packing of USO-16. Hydrogen atoms have been omitted for clarity. Green and blue polyhedra represent $[UO_8]$ and $[SO_4]$, respectively. Gray circles represent carbon atoms, and blue circles represent nitrogen atoms.

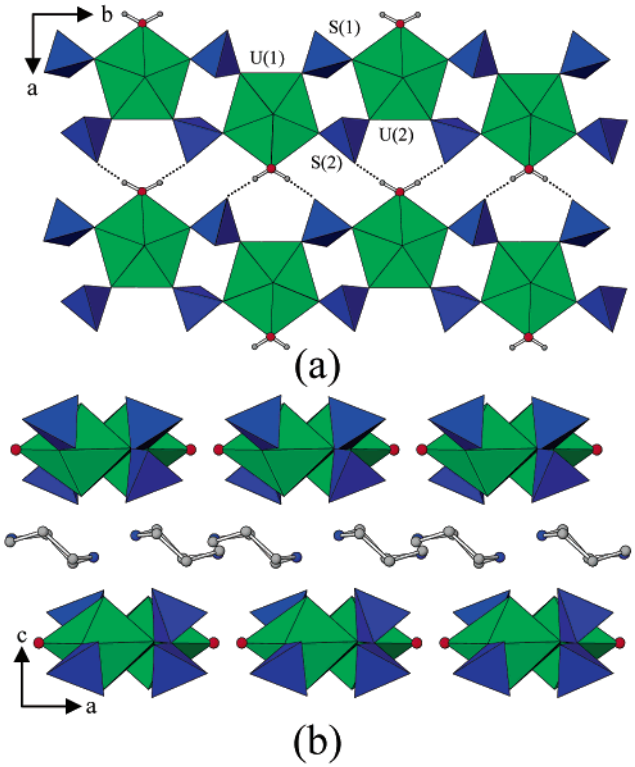

Figure 2. (a) One-dimensional $[UO_2(H_2O)(SO_4)_2]^{2-}$ chains in USO-18. Broken lines represent hydrogen bonds. (b) Three-dimensional packing in USO-18. Hydrogen atoms have been omitted for clarity. Green and blue polyhedra represent $[UO_7]$ and $[SO_4]$, respectively. Gray, blue, and red circles represent carbon, nitrogen, and oxygen atoms, respectively.

powder X-ray diffraction, with a total weight loss of 59.5% (calcd 64.6%).

USO-18. The inorganic chains and the three-dimensional packing are shown in Figure 2. Two distinct uranium centers are found in USO-18. Four of the five equatorial coordination sites around each uranium center bridge to sulfur centers, while the fifth is occupied by a bound water molecule. Two crystallographically distinct sulfur sites are observed in USO-18. Each sulfate tetrahedron bridges between two uranium polyhedra to form $[UO_2(H_2O)(SO_4)_2]^{2-}$ chains which run along the *b* axis. The bound water molecules (O(5) and O(6)) each donate hydrogen bonds to the sulfate tetrahedra of the adjacent chain, through a distance of 2.734(7) Å. This chain topology has been observed previously in the inorganic phases $Mn[(UO_2)(SO_4)_2(H_2O)]\cdot 4H_2O$[20] and $[(UO_2)(H_2PO_4)_2(H_2O)](H_2O)_2$,[21] and in USO-1,[8c] USO-3,[8d] USO-9,[8f] USO-11,[8g] and USO-22.[8r] $[hpipH_2]^{2+}$ cations reside between the inorganic chains, serving to balance the charge.

Template N−H bands are observed between 2750 and 3250 cm^{-1}, as is a sharp N−H band at 1612 cm^{-1} in the infrared spectrum. C−H bands are observed at 1420 and 1464 cm^{-1}. S−O bands are between 1000 and 1200 cm^{-1}, with the uranyl asymmetric stretch at 912 cm^{-1}.

A 3.3% weight loss, corresponding to the loss of the bound water molecule, is observed between 210 and 270 °C (calcd 2.6%) using thermogravimetric analysis. Weight losses between 280 and 480 °C and 480 and 900 °C correspond to loss of the template and decomposition of the inorganic structure. The material calcines to UO_2, as determined using powder X-ray diffraction, with a weight loss of 50.8% (calcd 53.4%).

USO-19. The structures of the inorganic layer and the three-dimensional packing are shown in Figure 3. There is a single U^{6+} center in USO-19. Each equatorial oxide bridges to one of two distinct sulfur environments in USO-19. Each tetrahedron connects two uranium polyhedra; however, the connectivities vary. The S(1) tetrahedra share two vertices with uranium polyhedra, whereas the S(2) polyhedra share a vertex and an edge. This forms $[UO_2(SO_4)_2]^{2-}$ layers, in the *ab* plane, of the type observed in the methylphosphonate, UPNO-2.[22]

$[dmedH_2]^{2+}$ templates lie between the layers, balancing the charge of the layers and donating hydrogen bonds to the layer. N(1) donates a hydrogen bond to O(8) through a distance of 2.723(9) Å. N(2) participates in extensive hydrogen bonding with the framework, through bonds to O(5), and O(9) and O(10) from layers above and below, through distances between 2.820(9) and 2.969(9) Å.

Template N−H bands are observed as a broad peak centered on 3156 cm^{-1} in the infrared spectrum, with a

(20) Tabachenko, V. V.; Balashov, V. L.; Kovba, L. M.; Serezhkin, V. N. *Koord. Khim.* **1984**, *10*, 854.
(21) Krogh-Anderson, E.; Krogh-Anderson, I. G.; Ploug-Sorensen, G. Structure Determination of a Substance Alleged to be Hendecahydrogen Diuranyl Phosphate. Presented at Solid State Materials for Low to Medium Temperature Fuel Cells and Monitors with Special Emphasis on Protonic Conductors: 3rd European Workshop. Solid State Protonic Conductors: For Fuel Cells and Sensors, Odense University, Odense, Denmark, 1985; p 192.
(22) Doran, M. B.; Norquist, A. J.; O'Hare, D. *Chem. Mater.* **2003**, *15*, 1449.

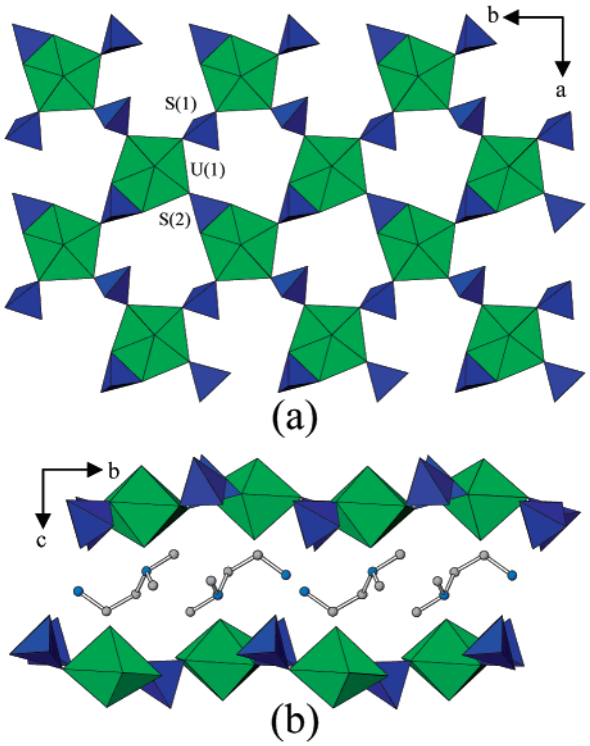

Figure 3. (a) Two-dimensional $[UO_2(SO_4)_2]^{2-}$ layers in USO-19. (b) Three-dimensional packing in USO-19. Hydrogen atoms have been omitted for clarity. Green and blue polyhedra represent $[UO_7]$ and $[SO_4]$, respectively. Gray circles represent carbon atoms, and blue circles represent nitrogen atoms.

sharper peak at 1606 cm^{-1}. C−H stretches are observed between 1458 and 1518 cm^{-1}. S−O bands are observed between 1000 and 1200 cm^{-1}, with a uranyl asymmetric stretch at 920 cm^{-1}.

USO-19 is thermally stable up to 320 °C using thermogravimetric analysis. Weight losses between 320 and 490 °C and 490 and 800 °C correspond to the loss of template and the decomposition of the inorganic structure. USO-19 calcines to UO_2, as determined using powder X-ray diffraction, with a weight loss of 50.1% (calcd 51.2%).

USO-20. The structure of the inorganic layer and the three-dimensional packing are shown in Figure 4. Two U^{6+} sites are present in USO-20. U(1) is bound to four equatorial oxide ligands from sulfate groups and one bound water molecule. U(2) is bound to five equatorial oxide ligands that bridge to sulfur centers. Three distinct sulfur sites are found in USO-20. Each tetrahedron is connected to three uranium polyhedra through vertices, forming $[(UO_2)_2(H_2O)(SO_4)_3]^{2-}$ layers in the *ab* plane. The layer topology has been seen in USO-2.[8c]

$[dmedH_2]^{2+}$ templates lie between the layers, balancing their charge and donating hydrogen bonds. N(1) donates a hydrogen bond to O(15) through a distance of 2.941(13) Å. N(2) donates hydrogen bonds to O(15), O(16), and O(18) through distances of 2.784(13), 2.920(13), and 2.733(13) Å, respectively.

Template N−H bands are observed as a set of broad peaks centered at 3454 cm^{-1}, and a peak at 1642 cm^{-1}, in the infrared spectrum. C−H bands are observed at 1458 and 1530 cm^{-1}. S−O bands are observed between 1000 and 1200 cm^{-1}. The asymmetric uranyl stretch is observed at 930 cm^{-1}.

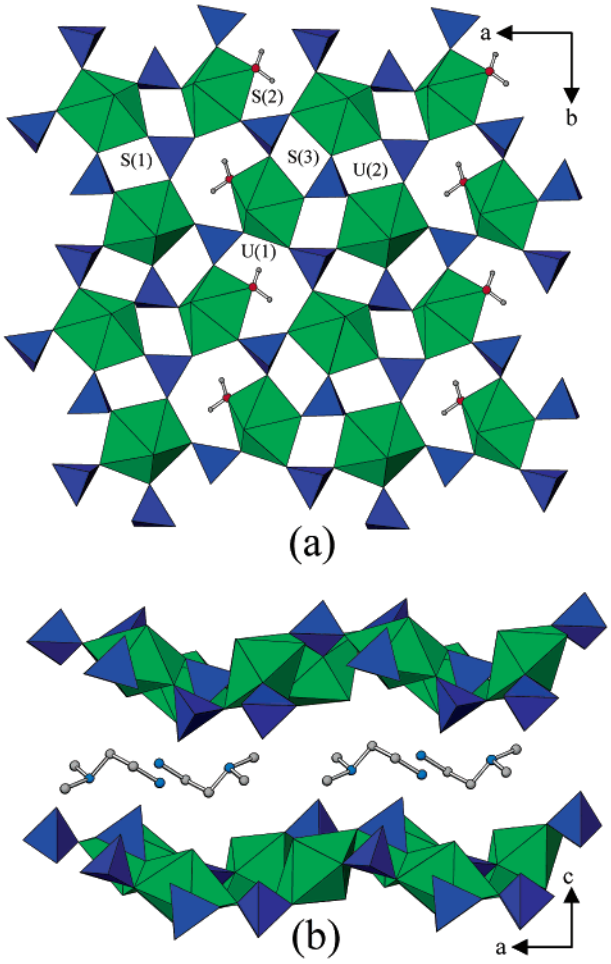

Figure 4. (a) Two-dimensional $[(UO_2)_2(H_2O)(SO_4)_3]^{2-}$ layers in USO-20. (b) Three-dimensional packing in USO-20. Hydrogen atoms have been omitted for clarity. Green and blue polyhedra represent $[UO_7]$ and $[SO_4]$, respectively. Gray, blue, and red circles represent carbon, nitrogen, and oxygen atoms, respectively.

A 1.6% weight loss between 154 and 206 °C and a further 2.2% weight loss between 210 and 255 °C correspond to loss of occluded and bound water (calcd 1.9% and 1.9%), respectively. Weight loss between 300 and 480 °C corresponds to decomposition of the template and breakdown of the inorganic structure. The material calcines to UO_2, as determined using powder X-ray diffraction, with a total weight loss of 42.4% (calcd 43.5%).

Composition Space Diagrams. In a composition space diagram, the compositions of the crystalline products are plotted as a function of the reactant mole fractions in the ternary composition space. The total number of moles of the three reactants, $UO_2Ac_2 \cdot 2H_2O$, template, and H_2SO_4, are held constant at all points. Any amorphous solids or soluble species after reaction are neglected. Areas of selective crystallization or "crystallization fields" are often observed. These diagrams are similar to ternary phase diagrams in that products are related to initial reactant compositions in a three-component system. However, the final composition is not necessarily the same as the initial composition; therefore, composition space diagrams are not phase diagrams as they do not obey the phase rule.

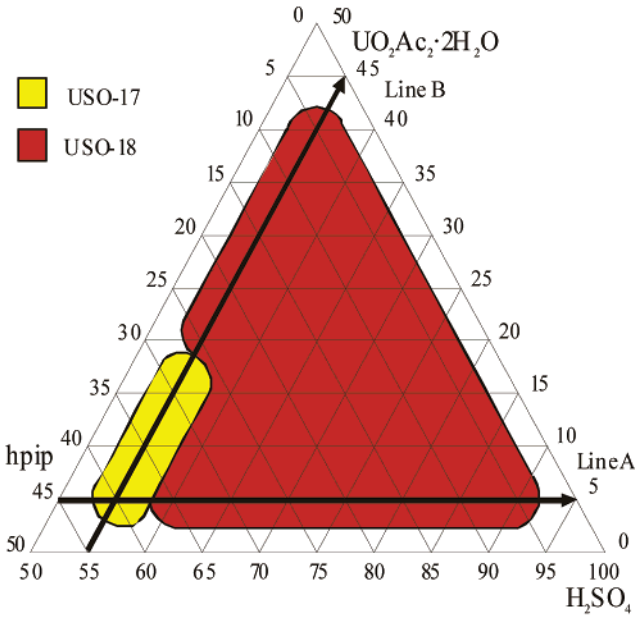

Figure 5. Composition space diagram for the $[UO_2Ac_2{\cdot}2H_2O/hpip/H_2SO_4]$ system. The scale on each axis represents the relative mole fraction of the corresponding component.

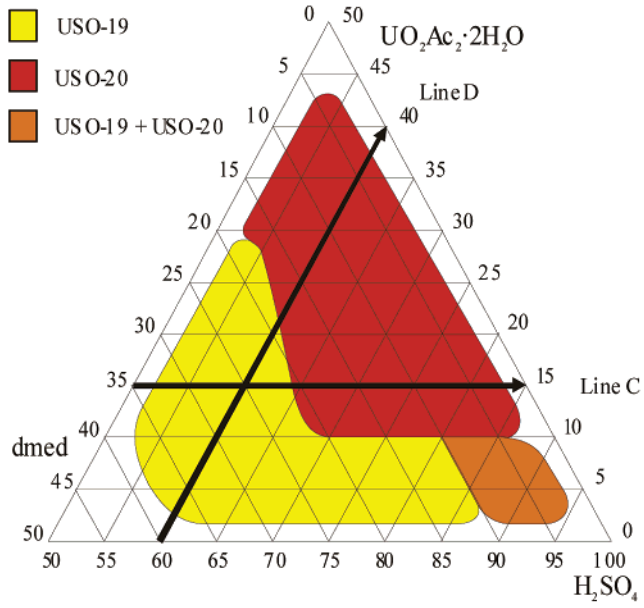

Figure 6. Composition space diagram for the $[UO_2Ac_2{\cdot}2H_2O/dmed/H_2SO_4]$ system. The scale on each axis represents the relative mole fraction of the corresponding component.

Each composition space was constructed by conducting 15−20 separate reactions. Reactant mole fractions were systematically varied; however, a constant number of moles was present in each reaction, 5 mmol. Reactions were restricted to acid rich conditions, H_2SO_4 mole fractions ≥ 0.5, because in other regions incomplete dissolution of starting materials or decomposition of template is observed. A constant amount of solvent water was added for each system (1 and 0.5 g, respectively, for the hpip and dmed containing systems).

The composition space diagram for the $[UO_2Ac_2{\cdot}2H_2O/hpip/H_2SO_4]$ system is shown in Figure 5. Two crystallization fields are observed, corresponding to USO-17 and USO-18. USO-17 is formed in the area of the composition space with high hpip mole fraction, between 32% and 47%, with a H_2SO_4 mole fraction between 53% and 58%. USO-18 forms in the remainder of the composition space.

The composition space diagram for the $[UO_2Ac_2{\cdot}2H_2O/dmed/H_2SO_4]$ system is shown in Figure 6. Three crystallization fields are observed, corresponding to USO-19, USO-20, and an area where the two phases cocrystallize. USO-20 forms in areas with high $UO_2Ac_2{\cdot}2H_2O$ mole fractions and low dmed mole fractions. In the region of highest acid concentration, USO-19 and USO-20 cocrystallize. USO-19 is the dominant product over the remainder of the composition space.

Discussion

$UO_2Ac_2{\cdot}2H_2O/hpip/H_2SO_4$ System. Two series of reactions are discussed, each with one reactant concentration held constant, in order to understand relative phase stabilities.

Line A (Figure 5) represents a series of reactions in which the $UO_2Ac_2{\cdot}2H_2O$ mole fraction is held constant at 5%. The conditions along line A range from hpip rich and H_2SO_4 deficient to hpip deficient and H_2SO_4 rich. At the hpip rich end of line A, the reaction product is USO-17. An increase in the H_2SO_4 concentration, with subsequent decrease in the hpip concentration, results in a shift in the reaction product from USO-17 to USO-18. This can be understood through inspection of the product compositions. USO-17, $[N_2C_5H_{14}]_2[UO_2(SO_4)_3]$, has a hpip:$[SO_4]^{2-}$ ratio of 2:3, whereas USO-18, $[N_2C_5H_{14}][UO_2(H_2O)(SO_4)_2]$, has the ratio 1:2. At the hpip rich end of line A, USO-17 is formed as the reagent concentrations more closely match the composition of the product with respect to USO-18. As the relative $[SO_4]^{2-}$ concentration increases, a shift to USO-18 is observed. This is because the elevated $[SO_4]^{2-}$ concentrations in solution are better mirrored by USO-18, a compound that is $[SO_4]^{2-}$ rich with respect to USO-17.

Line B (Figure 5) represents a series of reactions conducted at a constant $[SO_4]^{2-}$ mole fraction of 55%. At the hpip rich end of line B, USO-17 is observed, with USO-18 becoming the stable phase as the uranium concentration increases. The U:hpip ratio is 1:2 for USO-17 and 1:1 for USO-18. Thus, as the $[UO_2]^{2+}$ concentration increases, and the hpip concentration decreases, USO-18 becomes the stable phase, reflecting its higher U:hpip ratio as compared to USO-17.

$UO_2Ac_2{\cdot}2H_2O/dmed/H_2SO_4$ System. Two series of reactions are discussed, each with one reactant concentration held constant, in order to understand relative phase stabilities.

Line C (Figure 6) represents a series of reactions conducted at a constant $UO_2Ac_2{\cdot}2H_2O$ mole fraction of 15%. At the dmed rich end of line C, the reaction product is USO-19. As the $[SO_4]^{2-}$ concentration increases, the product shifts to USO-20. USO-19, $[N_2C_4H_{14}][UO_2(SO_4)_2]$, has a dmed:$[SO_4]^{2-}$ ratio of 1:2, whereas USO-20, $[N_2C_4H_{14}][(UO_2)_2(H_2O)(SO_4)_3]{\cdot}H_2O$, has the ratio 1:3. USO-19 is the stable phase in template rich conditions, and USO-20 is the stable phase in $[SO_4]^{2-}$ rich conditions, because their respective formulas mirror these reaction conditions.

Line D (Figure 6) represents a series of reactions conducted at a constant H_2SO_4 concentration. USO-19 is the reaction product in $[UO_2]^{2+}$ deficient conditions. A shift in product to USO-20 as the $[UO_2]^{2+}$ concentration increases is observed. This is explained through inspection of the template:U ratios of the two compounds. USO-19 has a dmed:U ratio of 1:1, compared with 1:2 in USO-20. This explains the formation of USO-20 over USO-19 in $[UO_2]^{2+}$ rich conditions.

Conclusion

Four new organically templated uranium sulfates have been synthesized from reactions in the [$UO_2Ac_2 \cdot 2H_2O$/homopiperazine/H_2SO_4] and [$UO_2Ac_2 \cdot 2H_2O$/*N*,*N*-dimethylethylenediamine/H_2SO_4] systems. Composition space has been used to elucidate the factors governing phase stability in four new organically templated uranium sulfates. It has been shown that the composition of the crystalline phases obtained from these series of hydrothermal reactions is dependent upon the composition of the reaction gel.

Acknowledgment. The authors thank the EPSRC for support.

Supporting Information Available: X-ray crystallographic file (CIF) containing complete tables of atomic coordinates, thermal parameters, and bond lengths and angles. Supplementary figures of thermal ellipsoid plots. TGA traces. This material is available free of charge via the Internet at http://pubs.acs.org.

IC034540J